Available online at www.sciencedirect.com

SciVerse ScienceDirect

Ceramics International 39 (2013) 1037–1044

CERAMICS INTERNATIONAL

www.elsevier.com/locate/ceramint

Microstructure and oxidation resistance of C-$AlPO_4$–mullite coating prepared by hydrothermal electrophoretic deposition for SiC–C/C composites

Kai-Tong Wang, Li-Yun Cao, Jian-Feng Huang*, Jie Fei, Bo-Ye Zhang

Key Laboratory of Auxiliary Chemistry and Technology for Chemical Industry, Ministry of Education, School of Material Science and Engineering, Shaanxi University of Science and Technology, Xi'an, Shaanxi 710021, PR China

Received 6 June 2012; received in revised form 4 July 2012; accepted 4 July 2012
Available online 20 July 2012

Abstract

Oxidation resistant C-$AlPO_4$–mullite coating for SiC pre-coated carbon/carbon composites (SiC–C/C) was prepared by a novel hydrothermal electrophoretic deposition process. The phase composition, surface and cross-section microstructure of the as-prepared multi-layer coatings were characterized by X-ray Diffraction (XRD), scanning electron microscopy (SEM) and energy dispersive spectroscopy (EDS). The influence of deposition voltage on phase composition, microstructure and oxidation resistance of the as-prepared coatings was particularly investigated. Results show that the outer layer coating mainly composed of C-$AlPO_4$ and mullite phase can be achieved after the hydrothermal electrophoretic deposition. The thickness, density and anti-oxidation property of the C-$AlPO_4$–mullite coating was improved with the increase of deposition voltage from 160 V to 200 V. The multi-layer coating prepared at a voltage of 200 V exhibit excellent anti-oxidation property, which can effectively protect C/C composites from oxidation in air at 1773 K for 324 h with a weight loss of 1.01%. The failure of the multi-layer coatings is due to the generation of cross-holes in the coating, which cannot be self-cured by the metaphosphate and silicate glass layer after long time oxidation at 1773 K.

Keywords: Mullite; Carbon/carbon composites; C-$AlPO_4$; Hydrothermal electrophoretic deposition

1. Introduction

Carbon/carbon (C/C) composites and carbon/carbon silicon carbide (C/C–SiC) composites possess many attractive properties, such as light weight, good thermal shock resistance and excellent mechanical properties [1–4]. They are thus outstanding candidate materials for use as high temperature structural components. The major advantage of C/C materials for high temperature application is that they do not lose strength as the temperature increases [2]. Consequently, C/C composites are considered as one of the most promising thermal-structural materials with many applications, such as on the nose caps and leading edges of space vehicles, disk brakes, turbine engines and so on [4–7]. Nevertheless, when the temperature reaches 723 K in the oxygen-containing atmosphere, the oxidation of C/C composites will limit their application [8–11]. Therefore, it is important to enhance the oxidation resistance of C/C composites to improve the usefulness in an oxidizing environment.

Multilayer coatings are considered as one of the best choices to protect C/C composites from oxidation at high temperature [10,12]. SiC ceramic coating usually be used as one of the best bonding layers for C/C composites because of its good physical and chemical compatibility with the C/C matrix [6,9]. Unfortunately, microcracks can be developed due to the mismatch of thermal expansion coefficient between SiC and C/C substrate, which cannot be self-cured by themselves [13]. In order to solve this problem, mulit-layer protective coatings technology is designed to seal the cracks on the SiC coating, such as SiC/$CrSi_2$ [5], $MoSi_2$/SiC [14], SiC nanowire-toughened SiC/$MoSi_2$ [15] and SiC–$MoSi_2$–$(Ti_{0.8}Mo_{0.2})Si_2$ [16]

---

*Corresponding author. Tel./fax: +86 029 86168802.
E-mail addresses: wangkaitong2006@126.com (K.-T. Wang), hjfnpu01@163.com (J.-F. Huang).

0272-8842/$ - see front matter © 2012 Elsevier Ltd and Techna Group S.r.l. All rights reserved.
http://dx.doi.org/10.1016/j.ceramint.2012.07.024

multi-layer coating. However, microcracks can be further developed due to the mismatch of thermal expansion coefficient between the SiC coating and outer coating, which lead to the decrease in oxidation resistance of the multi-coating.

As a result of its high melting point, good stability, lower oxygen permeability at high temperature, and good erosion resistance, mullite ($3Al_2O_3 \cdot 2SiO_2$) is a promising candidate material for the outer coating material [17–19]. In addition, the good match of thermal expansion coefficient and good physical and chemical compatibility between mullite ($4.4–5.6 \times 10^{-6}\,°C^{-1}$) and SiC ($4.3–5.4 \times 10^{-6}\,°C^{-1}$) [20] offer another advantage for adoption of mullite as outer coating material. The properties of cristobalite aluminum phosphate (C-$AlPO_4$) make it a promising candidate material for high temperature applications. These can be summarized as high melting point, low Young's modulus, low oxygen permeability and good erosion resistance. Besides, its thermal expansion coefficient ($5.5 \times 10^{-6}\,°C^{-1}$) is close to that of SiC ($4.3–5.4 \times 10^{-6}\,°C^{-1}$) and it has good chemical and physical compatibility to SiC, which will result in less defects and oxidation activity sites in matrix [21]. However, the traditional technologies, such as chemical vapor deposition [19,22] and pack cementation [2,4] are either high-cost or time-consuming. Hydrothermal electrophoretic deposition has been demonstrated to be a good low temperature method to deposit coatings such as yttrium silicates [23] and mullite [24] coatings with high performance. Up to now, few literature had concerned about using hydrothermal electrophoretic deposition process to prepare C-$AlPO_4$–mullite coating.

In the present work, an improved C-$AlPO_4$–mullite coating on SiC–C/C substrate was firstly prepared by a novel hydrothermal electrophoretic deposition process. The phase composition, morphology, oxidation resistance and failure mechanism of as-prepared C-$AlPO_4$–mullite/SiC multilayer were particularly investigated.

2. Experimental

2.1. Preparation of C-$AlPO_4$–mullite coating

Bulk 2D C/C composites with a density of 1.747 g/cm^3 were cut into small specimens ($10 \times 10 \times 10$ mm^3) to be used as substrates. The specimens were hand-polished using 300 grit SiC paper, then cleaned with distilled water and dried at 333 K for 2 h. The SiC coating was then applied through the pack cementation procedure. Details for the preparation of the inner SiC coating were reported in Ref. [25].

For the hydrothermal electrophoretic deposition process, C-$AlPO_4$ and mullite powders with the mass ratio of C-$AlPO_4$/mullite = 4:6 were dispersed in 170 ml isopropanol with an ultrasonic bath for 30 min (ultrasonic power was kept at 200 W) with a later magnetic stirring for 24 h. Iodine, used as a charging agent, was added into the suspension with another ultrasonic bath for 30 min (ultrasonic power was kept at 200 W) followed by constant magnetic stirring for 24 h. Next, the above suspension was transferred into a hydrothermal autoclave reported in Ref. [24,25].The anode of the autoclaves was a graphite substrate ($20 \times 10 \times 3$ mm^3) and the SiC–C/C substrate was fixed to the cathode of the autoclave. After being sealed, the autoclave was put into a furnace and the deposition voltage was kept at 160, 180, 200 or 220 V respectively. During the deposition process, the temperature was kept at 373 K. After 15 min of deposition, the autoclave was taken out of the furnace and cooled down naturally to room temperature. Then, the samples were dried at 333 K in air for 4 h. Finally, the homogeneous C-$AlPO_4$–mullite coating coated SiC–C/C composites was achieved.

2.2. Characterization

The phase composition of the coatings was measured with Rigaku D/max-3C X-ray diffraction (XRD) equipment operated at 40 kV and 100 mA with Cu Kα radiation ($\lambda = 0.15406$ nm) at a scanning rate of 8 min^{-1}. The morphology and element distribution of the multi-coating were analyzed using a JEOL JSM-6390A scanning electronic microscope (SEM) and energy dispersive spectroscopy (EDS). The bonding strength of the specimens was carried out in a universal material testing machine (PT-10369C). Six samples for each kind of samples were tested and the final bonding strength was obtained by computing the average values of six samples. The isothermal oxidation tests of the coated samples were carried out at 1773 K in an electrical furnace. The cumulative weight change of the samples after each thermal cycle was measured by an electrical balance with a sensitivity of ± 0.1 mg. The mass loss was calculated by Eqs. (A.1)–(A.3).

Where m_0 is the original mass of the coated C/C composites, m_1 is the mass of the coated C/C composites after oxidation at high temperature for certain time, t is oxidation time and the s is surface area of the specimen.

3. Results and discussion

3.1. Phase and microstructure of the multi-layer coatings

The surface XRD patterns (show in Fig. 1) of C-$AlPO_4$–mullite coating on SiC–C/C composites deposited at different voltages show peaks that only belong to C-$AlPO_4$ and mullite at all four voltages. This is accord with the original phase composition of the C-$AlPO_4$ and mullite powders. Additionally, the peak intensity of the C-$AlPO_4$ and mullite increase with the increase of deposition voltage, and when the deposition voltage reaches 220 V, the strongest C-$AlPO_4$ and mullite peaks are obtained. This may be attributed to the higher diffusion velocity of the charged C-$AlPO_4$ and mullite particles from the cathode to anode at higher deposition voltage, which is helpful for the increase of the coating thickness and will lead to the improvement in crystallization of C-$AlPO_4$–mullite coating.

Fig. 2 shows surface SEM images of the C-$AlPO_4$–mullite coating on SiC–C/C composites deposited at different voltages. Obviously, the coating surface of all the samples is composed of C-$AlPO_4$ and mullite crystallites with some microholes, but no cracks in the coating surfaces are observed. With the increase in deposition voltage from 160 V to 220 V, the surface of the coatings exhibits different morphologies. Loose coating is obtained at 160 V (Fig. 2a), inhomogeneous and porous C-$AlPO_4$–mullite coating is generated at 180 V (Fig. 2b), and very dense and homogeneous C-$AlPO_4$–mullite coating is achieved at 200 V (Fig. 2c). However, when the deposition voltage reaches 220 V (Fig. 2d), the as-prepared coating shows an inhomogeneous and porous morphology. This is possibly caused by high pressure conditions which provide sufficient energy for the dissolution, re-crystallization and growth of C-$AlPO_4$ and mullite crystalline and result in the formation of larger crystallites.

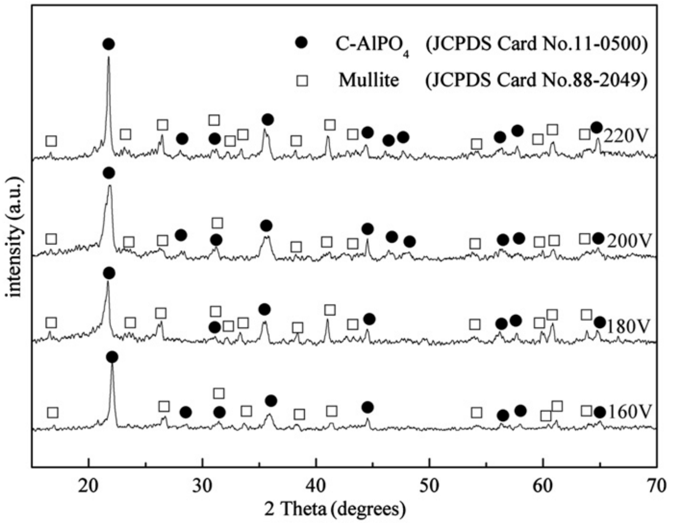

Fig. 1. Surface XRD patterns of C-$AlPO_4$–mullite coating on SiC–C/C composites deposited at different deposition voltages.

Cross-section SEM images of the C-$AlPO_4$–mullite coating deposited at different voltages is shown in Fig. 3. An obvious two-layer structure without microholes or penetrative cracks is achieved, which may be due to the good match in thermal expansion coefficient between the SiC bonding layer and the C-$AlPO_4$–mullite outer layer. As the increase of deposition voltage, the improvement in density and thickness of the C-$AlPO_4$–mullite coating is obvious. The thickness of the C-$AlPO_4$–mullite outer layer is about106.6, 159.8, 256.1 and 349.8 μm at the deposition voltages of 160, 180, 200 and 220 V, respectively. This indicates that the coating thickness increases with deposition voltage correspondingly, the improve in coating dense with the increase in deposition voltage is observed. Homogenous dense and crack-free multi-coating is achieved when the voltage is 200 V. Above 200 V, microcracks in the outer coating is found, which may due to the fast deposition and large thickness of the C-$AlPO_4$–mullite layer.

Fig. 4 shows the bonding strength of the as-prepared C-$AlPO_4$–mullite coatings deposited at different voltages clearly. The bonding strength between the outer layer coatings and C/C–SiC substrate increases with the increase of the deposition voltage from 160 V to 200 V. The bonding strength

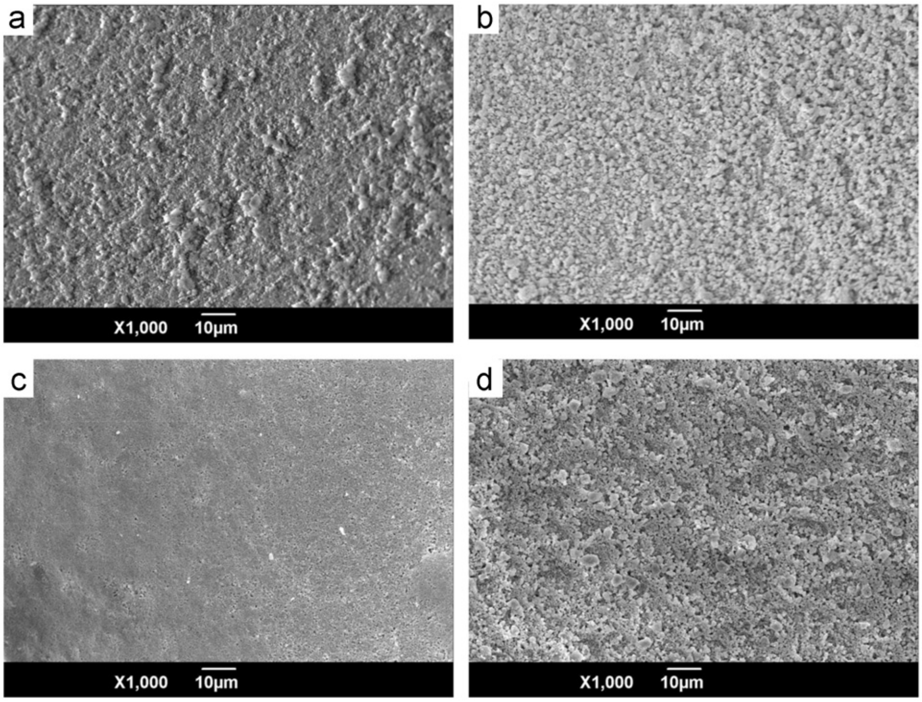

Fig. 2. Surface SEM images of the C-$AlPO_4$–mullite coating on SiC–C/C composites deposited at different deposition voltages. (a) 160 V; (b) 180 V; (c) 200 V and (d) 220 V.

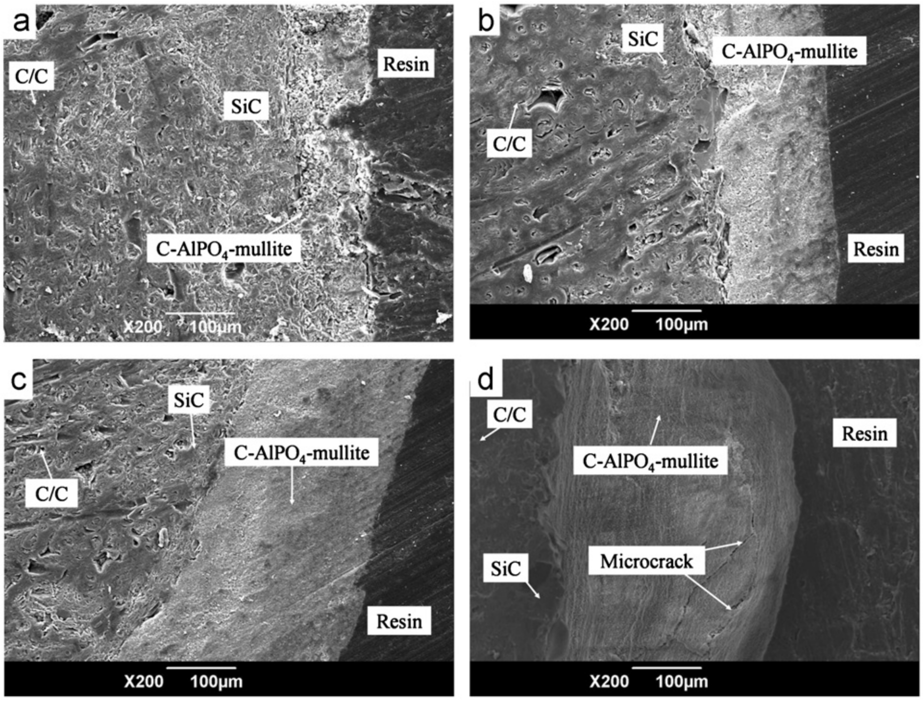

Fig. 3. Cross-section SEM images of the C-AlPO$_4$–mullite coating on SiC–C/C composites deposited at different deposition voltages. (a) 160 V; (b) 180 V; (c) 200 V and (d) 220 V.

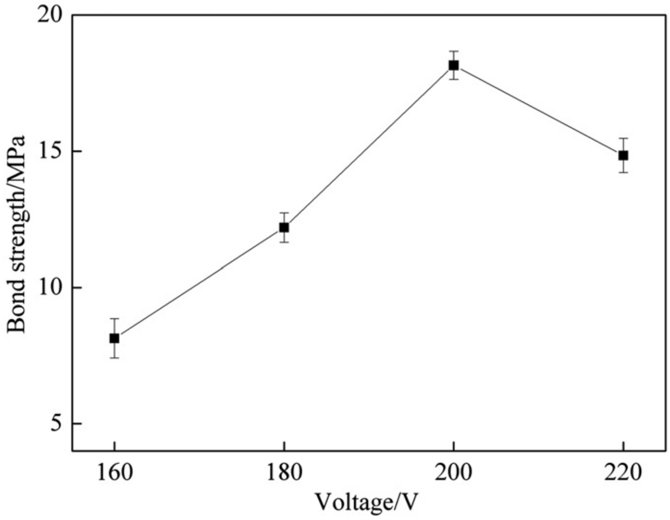

Fig. 4. Bonding strength of C-AlPO$_4$–mullite coatings prepared at different voltages by hydrothermal electrophoretic deposition.

between the C-AlPO$_4$–mullite coatings (deposited at 160 V)and C/C–SiC substrate is tested to be 8.14 MPa. When the deposition voltage reaches 180 V, The bonding strength arrives to 12.19 MPa. When the deposition voltage reaches 200 V, the highest bonding strength of 18.15 MPa between the C-AlPO$_4$–mullite coatings and C/C–SiC substrate is achieved, which is resulted from the homogeneous, crack-free and dense structure of C-AlPO$_4$–mullite coating (Figs. 2c, 3c). To be expected, the better oxidation resistance of C-AlPO$_4$–mullite coated SiC–C/C composites will be achieved. However, when the deposition voltage reaches 220 V, the bonding

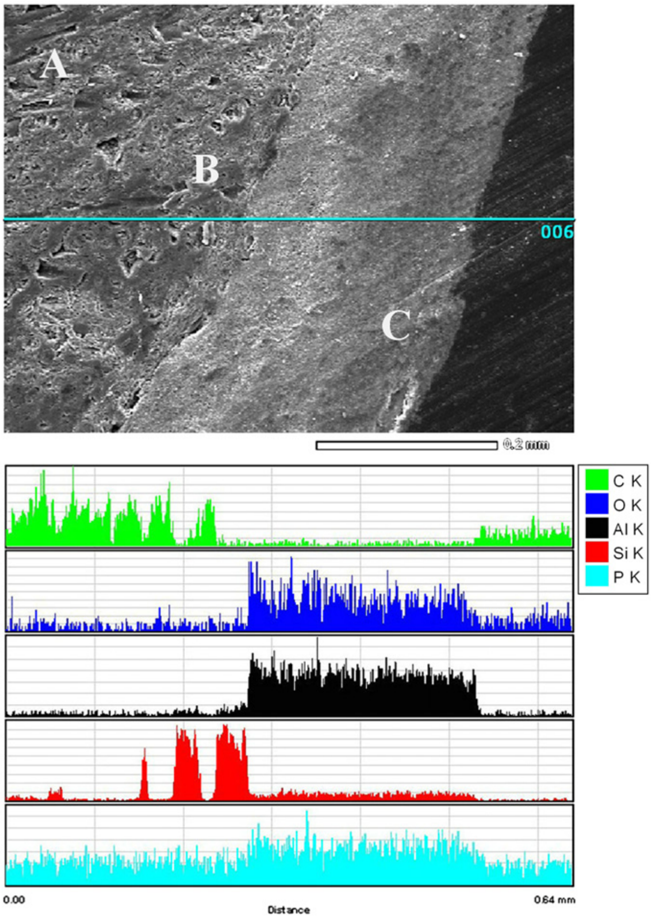

Fig. 5. Cross-section EDS element line scan analysis of C-AlPO$_4$–mullite/SiC multi-layer coating according to Fig. 3(c).

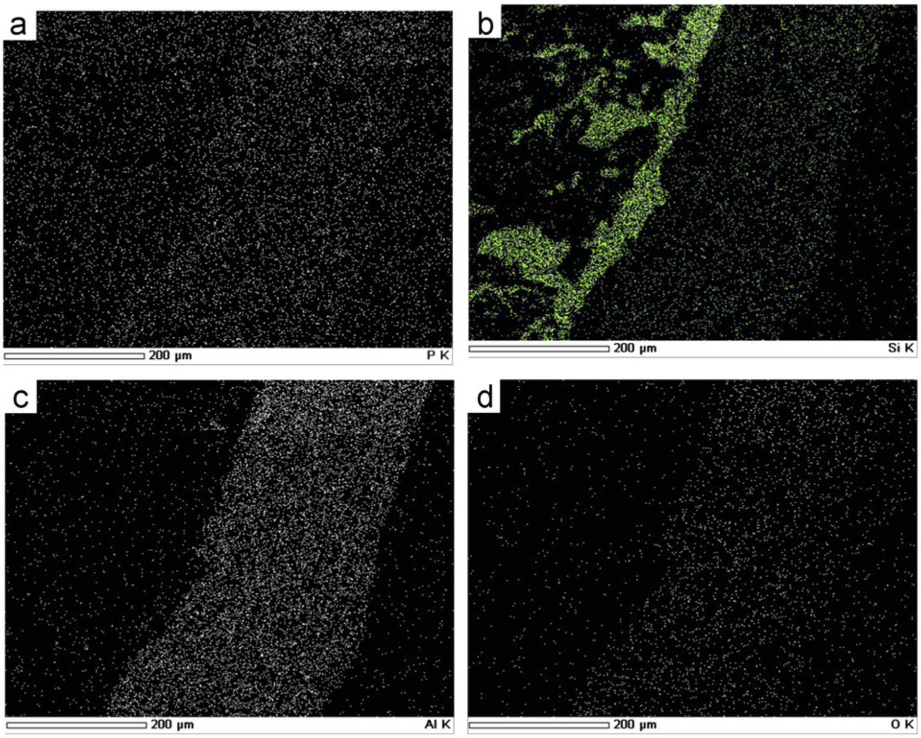

Fig. 6. Cross-section EDS element surface scan analysis of C-$AlPO_4$–mullite/SiC multi-layer coating according to Fig. 3(c). (a) P element distribution; (b) Si element distribution; (c) Al element distribution and (d) O element distribution.

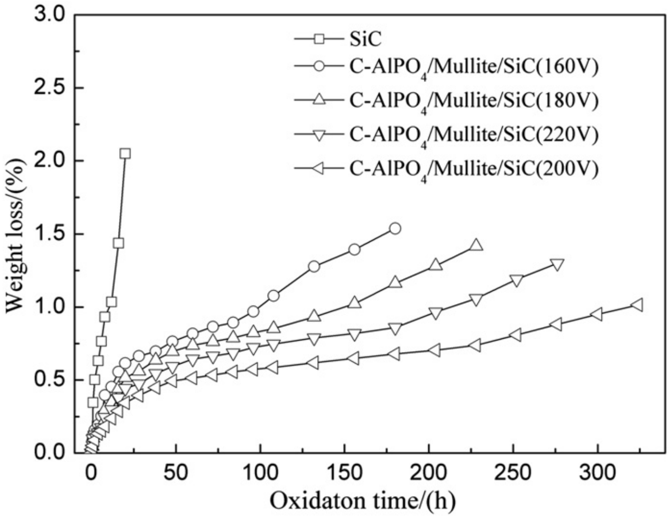

Fig. 7. Isothermal oxidation curves of SiC–C/C composites and the C-$AlPO_4$–mullite coating coated SiC–C/C composites in air at 1773 K.

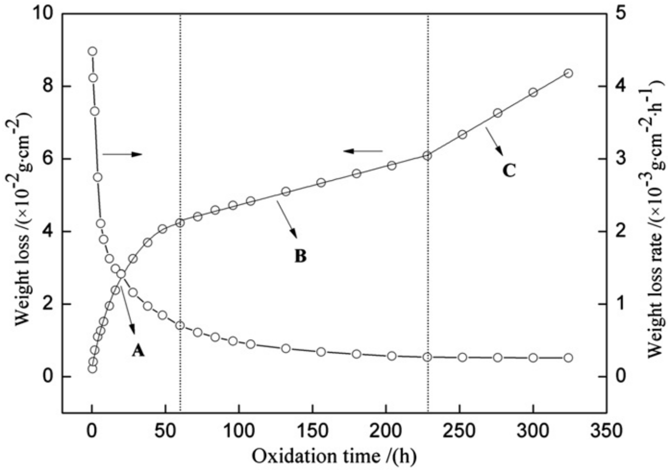

Fig. 8. Isothermal oxidation curve of the C-$AlPO_4$–mullite coating (deposited at 200 V) coated SiC–C/C composites in air at 1773 K.

strength will decrease to 14.84 MPa, which is resulted from the inhomogeneous and porous microstructure of C-$AlPO_4$–mullite coating (Figs. 2d, 3d). Therefore, it is inferred that the deposition voltage is the key factor for achieving dense and high bonding strength outer coating.

Fig. 5 displays the cross-section EDS element line scan analysis of the C-$AlPO_4$–mullite/SiC multi-layer coating, showing the concentration distributions of C, O, Al, Si and P element along the coating cross direction. The element line scan analysis shows that the multi-layer coating could be divided into three parts, designated as A, B and C. Part A is the carbon/carbon composites matrix infiltrated by Si, attributing to the pack cementation process. Part B is the SiC bonding layer, and part C is the C-$AlPO_4$–mullite coating that is well agreement with the experimental designation.

Fig. 6 displays the cross-section EDS element surface scan analysis of the C-$AlPO_4$–mullite/SiC multi-layer coating, showing the distributions status of P, Si, Al and O element in the coating. The distribution status of C-$AlPO_4$ and mullite has been given out in the coatings as shown in Fig. 6(a)–(d).

3.2. *Antioxidation property of the multi-layer coating*

The isothermal oxidation curves of SiC and the C-$AlPO_4$–mullite coating coated SiC–C/C composites in air at 1773 K are shown in Fig. 7. After oxidation in air for 20 h at 1773 K, the mass loss of SiC–C/C composites is about 2.04%, which infers that the single SiC coating cannot effectively protect C/C composites from oxidation for long time. Comparatively, the C-$AlPO_4$–mullite coated SiC–C/C composites exhibit much better anti-oxidation properties. The rate of mass loss decreases as the increase of thickness, homogeneity and density of C-$AlPO_4$–mullite coating. Thus, the improvement in anti-oxidation property is observed with increasing deposition voltage until 200 V. Corresponding to the generation of microcracks in outer coating, the decrease in oxidation resistance of the coated samples is found when the deposition voltage arrives to 220 V. For the sample prepared at 200 V, the mass loss is only 1.01% after 324 h oxidation at 1773 K. The oxidation protection ability is obviously improved and better than the reported Al_2O_3–mullite–SiC–Al_4SiC_4 multi-composition coating [4] and the mullite-SiC multi-coating [24].

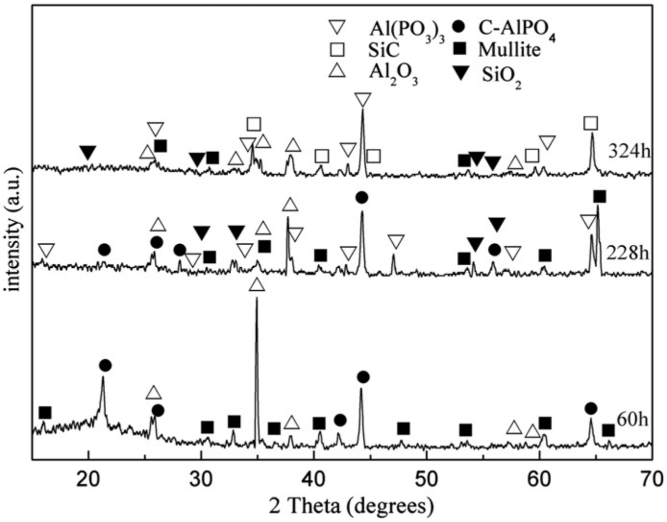

Fig. 9. Surface XRD patterns of the C-$AlPO_4$–mullite/SiC–C/C sample after oxidation at 1773 K in air for different hours.

Fig. 8 exhibits the isothermal oxidation curve of C-$AlPO_4$–mullite coating (deposited at 200 V) coated SiC–C/C composites in air at 1773 K. Obviously, the as-prepared C-$AlPO_4$–mullite coating can protect SiC–C/C composites from oxidation at 1773 K for 324 h with the weight loss of only 8.36×10^{-2} g cm^{-2} and the corresponding weight loss rate is 2.58×10^{-4} g cm^{-2} h^{-1}. The oxidation behavior of the coated sample can be divided into three processes marked as A, B, and C by the analyses of the oxidation curves.

Fig. 9 shows the XRD pattern of C-$AlPO_4$–mullite/SiC coated C/C composite oxidation at different times. It is suggested that the C-$AlPO_4$–mullite/SiC coated C/C composites mainly undergo the following eight reactions as shown in Eqs. (A.4)–(A.11) at high temperature.

At the initial oxidation stage (0–60 h), the weight loss of the sample with time follows a parabolic law and the obviously weight loss of sample is detected (process A). It is clear that the sample gain weight quickly to 4.24×10^{-2} g cm^{-2} during the initial 60 h oxidation. Additionally, by SEM observation, the coating's surface is harsh and rough with many microholes (Fig. 10a), which indicates that the

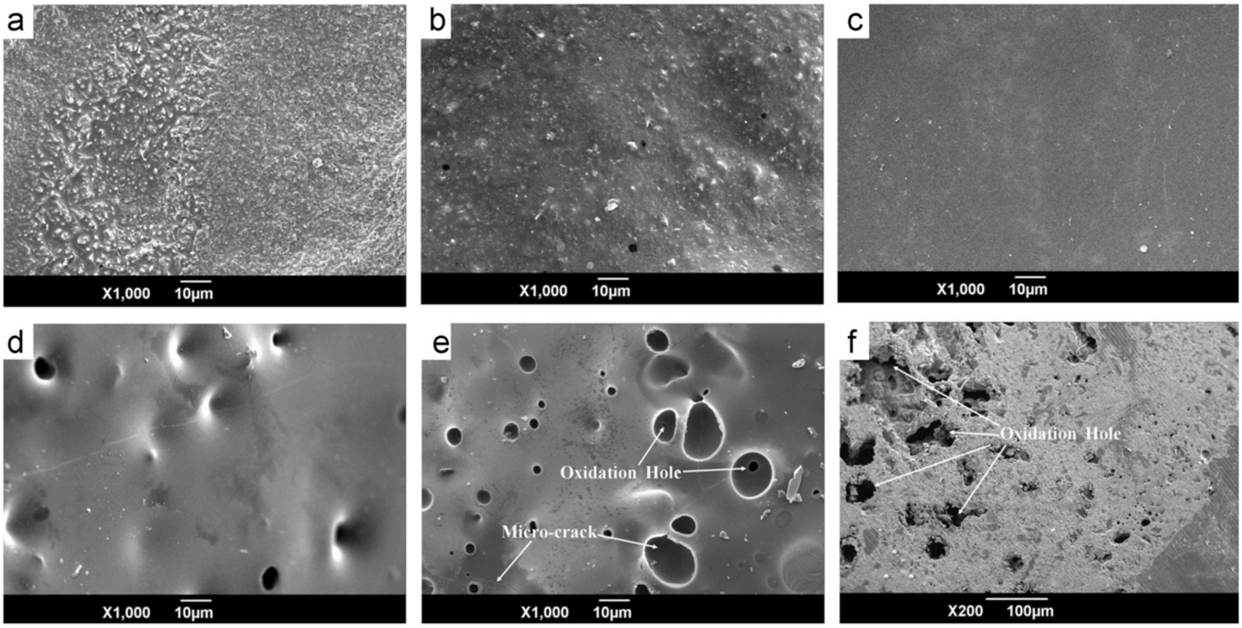

Fig. 10. Surface((a)–(e)) and cross-section (f) SEM images of C-$AlPO_4$–mullite coating on SiC–C/C composites after oxidation at 1773 K in air for different hours. (a) 28 h; (b) 60 h; (c) 228 h; (d) 276 h; (e) 324 h and (f) 324 h.

weight loss of the sample may due to the oxidation of C/C matrix through the microholes. During this oxidation stage, part of C-$AlPO_4$ exposes to air and decompose into Al_2O_3 and PO_x (Eq. (A.4)) with a later transformation into C-$AlPO_4$ molten phase (Eq. (A.5)). In the meantime, oxygen will diffuse along the microhole of the C-$AlPO_4$–mullite coating to the interface between the C-$AlPO_4$–mullite and SiC–C/C. As a result, the oxygen then will react with SiC (Eqs. (A.8), (A.9)) bonding layer.

As the increase of oxidation time, the C-$AlPO_4$–mullite outer layer can be gradually transformed into the metaphosphate (Eq. (A.6)) and silicate glass (Eq. (A.7)) layer [26] (Fig. 10b) and simultaneously the generation of Al_2O_3 is detected (Eq. (A.7), Fig. 9). From 60 h to 228 h (process B), the thicker metaphosphate and silicate glass layer can be completely formed (Fig. 10c), which will result in the good protection for the C/C matrix due to their low oxygen permeation constant and good self-cure ability (Fig. 10d). The average weight loss rate in this process keeps below 7.06×10^{-4} g cm^{-2} h^{-1}, which infers that the oxidation rate of the coated sample is mainly controlled by the diffusion rate of oxygen along the molten layer. After 228 h oxidation (process C) at 1773 K, the weight loss of the coated sample increase quickly with time, which may result from the volatilization of the glass layer and lead to the decrease in coating thickness. As a result, oxygen is able to diffuse through the thin metaphosphate and silicate glass layer and react with the C/C matrix as shown in Eqs. (A.10)–(A.11). These reactions will lead to the formation of microholes (Fig. 10d and e) in the glass layer due to the escape of CO and CO_2. At the same time, microcracks and oxidation holes (Fig. 10e and f) will also be generated in the coating, which may due to the frequent thermal shocks from high temperature to room temperature during the isothermal oxidation test. The as-generated microholes, microcracks and oxidation holes provide the channels for oxygen to attack the C/C matrix, which will lead to the decrease in oxidation resistance of the coated sample.

4. Conclusion

In conclusion, an improved dense and homogeneous C-$AlPO_4$–mullite coating for SiC–C/C composites was successfully prepared by a novel hydrothermal electrophoretic process at low temperature. The thickness, density and oxidation resistance of the as-prepared coating improve with the increase of deposition voltages from 160 V to 200 V. The bonding strength between the outer layer coatings and C/C–SiC matrix increases with the increase of the deposition voltage from 160 V to 200 V. The C-$AlPO_4$–mullite coating prepared at voltage of 200 V can effectively protect C/C composites from oxidation in air at 1773 K for 324 h with a weight loss of only 8.36×10^{-2} g cm^{-2}. The failure of the multi-layer coatings is attributed to the generation of microholes and microcracks due to the escape of CO and CO_2 and the volatilization of metaphosphate and silicate molten layer.

Acknowledgments

This work has been supported by the National Natural Science Foundation of China (51172134 and 51072108), Natural Science Foundation of Shaanxi province educational office (2010JK444) and the Graduate Innovation Foundation of Shaanxi University of Science and Technology.

Appendix A

$$WL\% = (m_0 - m_1)/m_0 \times 100\% \tag{A.1}$$

$$WL = (m_0 - m_1)/s \times 100\% \tag{A.2}$$

$$WLR = (m_0 - m_1)/st \times 100\% \tag{A.3}$$

$$\mathrm{C-AlPO_4}(s) \rightarrow \mathrm{Al_2O_3}(s) + \mathrm{PO}_x(g) \tag{A.4}$$

$$\mathrm{C-AlPO_4}(s) \rightarrow C\text{-}\mathrm{AlPO_4}(m) \tag{A.5}$$

$$3\mathrm{C-AlPO_4}(s) \rightarrow \mathrm{Al(PO_3)_3}(s) + \mathrm{Al_2O_3}(g) \tag{A.6}$$

$$\mathrm{SiO_2}(s) + 3\mathrm{Al_2O_3} \cdot 2\mathrm{SiO_2}(s) \rightarrow \mathrm{silicatesglass}(m) + \mathrm{Al_2O_3}(g) \tag{A.7}$$

$$\mathrm{SiC}(s) + \mathrm{O_2}(g) \rightarrow \mathrm{SiO}(g) + \mathrm{CO}(g) \tag{A.8}$$

$$\mathrm{SiC}(s) + 2\mathrm{O_2}(g) \rightarrow \mathrm{SiO_2}(s) + \mathrm{CO_2}(g) \tag{A.9}$$

$$2\mathrm{C}(s) + \mathrm{O_2}(g) \rightarrow 2\mathrm{CO}(g) \tag{A.10}$$

$$C(s) + \mathrm{O_2}(g) \rightarrow \mathrm{CO_2}(g) \tag{A.11}$$

References

[1] L.F. Cheng, Y.D. Xu, L.T. Zhang, X.W. Yin, Preparation of an oxidation protective coating for C/C composites by low pressure chemical vapor deposition, Carbon 38 (2000) 1493–1498.

[2] M. Huang, K.Z. Li, H.J. Li, Q.G. Fu, G.D. Sun, Double-layer oxidation protective SiC/Cr–Al–Si coating for carbon–carbon composites, Surface and Coatings Technology 18 (2007) 7842–7846.

[3] X.T. Shen, K.Z. Li, H.J. Li, Q.G. Fu, S.P. Li, F. Deng, The effect of zirconium carbide on ablation of carbon/carbon composites under an oxyacetylene flame, Corrosion Science 53 (2011) 105–112.

[4] J.F. Huang, X.R. Zeng, H.J. Li, X.B. Xiong, M. Huang, Al_2O_3–mullite–SiC–Al_4SiC_4 multi-composition coating for carbon/carbon composites, Materials Letters 58 (2004) 2627–2630.

[5] Q.G. Fu, H.J. Li, X.H. Shi, L.X. Ling, K.Z. Li, M. Huang, Microstructure and anti-oxidation property of $CrSi_2$–SiC coating for carbon/carbon composites, Applied Surface Science 10 (2006) 3475–3480.

[6] X.B. Xiong, X.R. Zeng, C.L. Zou, J.Z. Zhou, Strong bonding strength between HA and $(NH_4)_2S_2O_8$-treated carbon/carbon composite by hydrothermal treatment and induction heating, Acta Biomaterialia 5 (2009) 1785–1790.

[7] X.B. Xiong, X.R. Zeng, C.L. Zou, Preparation of enhanced HA coating on H_2O_2-treated carbon/carbon composite by induction heating and hydrothermal treatment methods, Materials Chemistry and Physics 114 (2009) 434–438.

[8] J.F. Huang, L.Y. Cao, Q. Mi, X.P. Yang, Influence of hydrothermal treatment temperature on oxidation modification of C/C composites with aluminum phosphates solution by a microwave hydrothermal process, Corrosion Science 52 (2010) 3757–3762.

[9] J.F. Huang, X.R. Zeng, H.J. Li, X.B. Xiong, G.L. Sun, ZrO_2–SiO_2 gradient multilayer oxidation protective coating for SiC coated carbon/carbon composites, Surface and Coatings Technology 2–3 (2005) 255–259.

[10] James E. Sheehan, Oxidation protection for carbon fiber composites, Carbon 27 (1989) 709–715.

[11] X.F. Qiang, H.J. Li, Y.L. Zhang, Q.G. Fu, J.F. Wei, S. Tian, A modified dual-layer SiC oxidation protective coating for carbon/carbon composites prepared by one-step pack cementation, Corrosion Science 53 (2011) 523–527.

[12] Y.L. Zhang, H.J. Li, X.Y. Yao, K.Z. Li, X.F. Qiang, Oxidation protection of C/SiC coated carbon/carbon composites with Si–Mo coating at high temperature, Corrosion Science 53 (2011) 2075–2079.

[13] Hiroshi Hatta, Takuya Aoki, Yasuo Kogo, Toshio Yarii, High-temperature oxidation behavior of SiC-coated carbon fiber-reinforced carbon matrix composites, Composites Part A Applied Science and Manufacturing 30 (1999) 515–520.

[14] J.F. Huang, B. Wang, H.J. Li, M. Liu, L.Y. Cao, C.Y. Yao, A $MoSi_2$/SiC oxidation protective coating for carbon/carbon composites, Corrosion Science 2 (2011) 834–839.

[15] Q.G. Fu, H.J. Li, K.Z. Li, X.H. Shi, Z.B. Hu, M. Huang, SiC whisker-toughened $MoSi_2$–SiC–Si coating to protect carbon/carbon composites against oxidation, Carbon 44 (2006) 1866–1869.

[16] G.S. Jiao, H.J. Li, K.Z. Li, C. Wang, D.S. Hou, SiC–$MoSi_2$–$(Ti_{0.8}Mo_{0.2})Si_2$ multi-composition coating for carbon/carbon composites, Surface and Coatings Technology 201 (2006) 3452–3456.

[17] T. Damjanovic, Chr. Argirusis, G. Borchardt, H. Leipner, R. Herbig, G. Tomandl, R. Weiss, Oxidation protection of C/C–SiC composites by an electrophoretically deposited mullite precursor, Journal of the European Ceramic Society 5 (2005) 577–587.

[18] Yahua Bao, Patrick S. Nicholson, $AlPO_4$-coated mullite/alumina fiber reinforced reaction-bonded mullite composites, Journal of the European Ceramic Society 16 (2008) 3041–3048.

[19] H. Fritze, J. Jojic, T. Witkeb, C. Rüscherc, S. Weberd, S. Scherrerd, R. Weiße, B. Schultrichb, G. Borchardta, Mullite based oxidation protection for SiC–C/C composites in air at temperatures up to 1900 K, Journal of the European Ceramic Society 16 (1998) 2351–2364.

[20] P.W.M. Peters, B. Daniels, F. Clemens, W.D. Vogel, Mechanical characterisation of mullite-based ceramic matrix composites at test temperatures up to 1200 °C, Journal of the European Ceramic Society 5 (2000) 531–535.

[21] J.F. Huang, W.D. Yang, L.Y. Cao, Preparation of a SiC/Cristobalite-$AlPO_4$ multi-layer protective coating on carbon/carbon composites and resultant oxidation kinetics and mechanism, Journal of Materials Science and Technology 26 (2010) 1021–1026.

[22] W. Kowbel, J.C. Withers, P.O. Ransone, CVD and CVR Silicon-based functionally gradient coatings on C–C composites, Carbon 33 (1995) 415–426.

[23] J.F. Huang, Y.T. Zhang, X.R. Zeng, L.Y. Cao, F. Deng, J.P. Wu, Hydrothermal electrophoretic deposition of yttrium silicate coating on SiC–C/C composites, Materials Technology 22 (2007) 85–87.

[24] J.F. Huang, Q. Yang, T. Yang, L.Y. Cao, Q.F. Zhang, Microstructure and anti-oxidation property of mullite oxidation protective coating prepared by hydrothermal electrophoretic deposition for SiC–C/C composites, Surface and Coatings Technology 205 (2011) 5077–5082.

[25] J.F. Huang, M. Liu, B. Wang, L.Y. Cao, C.K. Xia, J.P. Wu, SiC_n/SiC oxidation protective coating for carbon/carbon composites, Carbon 4 (2009) 1198–1201.

[26] T. Damjanovic, Chr. Argirusis, B. Jokanovic, G. Borchardt, K. Moritz, E. Müller, R. Herbig, R. Weiss, Oxidation protection of C/C–SiC composites by an electrophoretically deposited mullite precursor: Cyclic thermogravimetric analysis, Journal of the European Ceramic Society 27 (2007) 1299–1302.